NEXT STEPS IN WIND TUNNEL AEROACOUSTICS: MEASUREMENTS AT FLIGHT-REYNOLDS NUMBERS

Thomas Ahlefeldt
German Aerospace Center (DLR), Göttingen, Germany, thomas.ahlefeldt@dlr.de

In my talk I will present the microphone array measurement technique which was advanced at the DLR Göttingen for the use in cryogenic and/or pressurized wind tunnels [1]. This extends the range for acoustic measurements on scaled aircraft models in start and landing configuration up to real-flight Reynolds numbers. This abstract describes the measurements carried out in the European Transonic Wind Tunnel (ETW) and presents the results.
In the talk I will also give additional examples for measurements performed in a cryogenic wind tunnel [2-3] and give an insight in the comparability of microphone array measurements. In the example chosen, results obtained from the same model but different wind tunnels are being compared [4].

Motivation

The use of microphone arrays to acquire acoustic data of scaled models in wind tunnels has become a standard measurement technique. However, the comparison of the results obtained in the wind tunnel to those obtained at real flight tests usually reveals differences. These differences are attributable to a lack of model fidelity, installation effects, a discrepancy in Reynolds number, and the applicability of the assumptions made in phased array processing [5]. The work presented in the following is focused on the effect of varying Reynolds number.

Measurement setup

The ETW facility is a high Reynolds number transonic wind tunnel with a 2.0 m × 2.4 m closed test section. By injection of liquid nitrogen, the wind tunnel can be operated over a temperature range from 110 K up to 310 K and the total pressure can be varied between approximately 115 kPa and 450 kPa. Thereby the ETW provides a testing environment for full-scale Reynolds numbers and independent variation of Reynolds number, Mach number, and load [6].
Figure 1 shows the measurement setup with the half-model in high lift configuration (scale 1:13.6) in the center of the test section of the ETW. The positioning of the microphones was limited to discrete dummy windows and side wall slots as can be seen on the left side of Figure 1. For the sensors, Brüel & Kjær cryogenic-type sensor of type 4944A were used. This sensor was developed

together with the DLR and the ETW. The corresponding frequency response measurements at different pressures and temperatures were performed in a cryogenic vessel at the ETW site. They exhibited a non-linear combination of the amplitude response caused by varying the static pressure or temperature separately [1,7].
Measurements were taken for several Mach numbers, Reynolds numbers and angles of attack. In order to additionally assess the influence of the different load on the model at higher pressures (deformation), several measurement points were chosen to give the following features: (1) comparisons at same deformation but different Reynolds numbers, (2) comparisons at the same Reynolds number but different deformations. Thus, the effect of the elastic deformation can be separated from the effect of the Reynolds number.

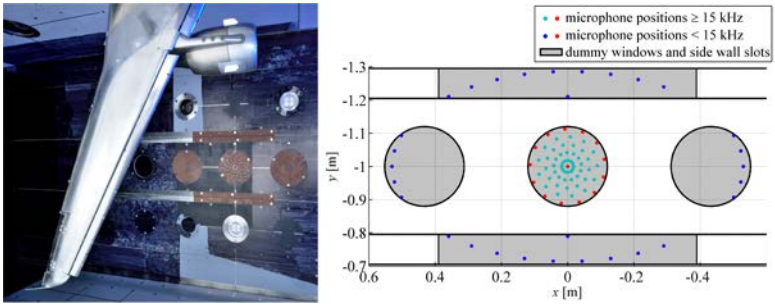

Fig. 1: Photo of the setup and arrangement of microphones.

Algorithms and Assumptions

For the reconstruction of the source auto powers on a chosen grid, the conventional beamforming approach in the frequency domain was used [8].
The limitation for the microphone positioning lead to strong side lobes in the beamforming procedure caused by insufficient spatial sampling. Here, results will be shown using the pseudo-deconvolution method CLEAN-SC [9].
For the calculation of the results, several assumptions are to be made. Independent of the cryogenic/pressurized environment, the phase shift of each reconstructed source was calculated using a point source assumption under homogeneous flow conditions.
For the comparison of results obtained at different temperatures and pressures, the influence of those quantities must be considered in terms of corrections. First, a correction is required to take into account the alteration of the radiated sound pressure caused by the different temperatures and pressures. This correction will be also dependent on the assumptions made for the nature of the source. Here, the main contributing kind of source from the half-model in the

test section is considered to be dipole sources [1]. This correction can be derived from the Ffowcs-Williams–Hawkings solution of the acoustic analogy with surface sources in the far-field. The resulting decibel correction for dipole sources with consideration of different temperatures and static pressures in the test section is given by (for details see [1]):

$$\Delta \text{ dB} = 20 \log_{10}\left(\frac{\rho a^2}{\rho_0 a_0^2}\right)$$

Here, the density is taken as $\rho_0 = 1.25$ kg⁄m^3 and the speed of sound as $a_0 = 337$ m⁄s (values for pure nitrogen at international standard atmosphere conditions). Second, as an additional normalization approach, the results are be compared at the same Strouhal number to account for the different flow velocities, where even the Mach numbers are still the same at these different temperatures and pressures.

With the application of these assumptions, differences found in a comparison can be related to source mechanisms not scaling as a compact dipole source or with the Strouhal number (i.e., Reynolds number effects, cavity or jet noise).

Experimental Results

The source maps were computed over an equidistant discrete grid with 69,165 grid points covering the region of interest in an observation plane of 1.30 × 1.32 m on the half-model. Exemplary results are shown in figure 2. It shows a comparison of results at Reynolds numbers of 1.43×10^6 and 20.06×10^6. In general, the source maps exhibit dominant sources at the inboard slats, slat tracks, and flap side edge, with less dominant sources at the flap and the flap track fairings. At a Strouhal number of 20 the source maps are almost equal showing the same source positions and the same level. However, for a Strouhal number of 130, the source map for the real-flight Reynolds number exhibits differences. Sources with a significantly increased noise level appear on the inner flap and on one flap fairing. The sources on the inner flap are the most dominant ones for the real flight Reynolds number case. On the other hand, the sources on the slat are significantly decreased.

For a closer observation, figure 3 shows spectra taken at an angle of attack of 3 deg. Each spectrum represents different areas on the wing, the slat and the flap area. The spectra were calculated by integrating the CLEAN-SC results over the grid points covering the slat or flap area.

For the comparison of the slat spectra one important effect of the Reynolds number can be observed: various slat tone peaks disappear for higher Reynolds numbers. These so called “slat tones” are related to different noise mechanisms occurring at the slat cove. They can be considered a model artifact due to too low Reynolds numbers and manufacturing and handling constraints [10].

The comparison of the flap sources also shows various differences for both Reynolds numbers. First, a hump is visible at a Strouhal number of 40, related to the flap side edge showing a slight shift of the Strouhal number as well as of its source strength. Of major significance are two large broadband increases appearing in the Strouhal number range of 100 to 150 and 170 to 200 at the flight Reynolds number. These humps are related to sources on the inboard flap (see figure 2) and the outboard flap showing a level increase of approximately 10 dB.

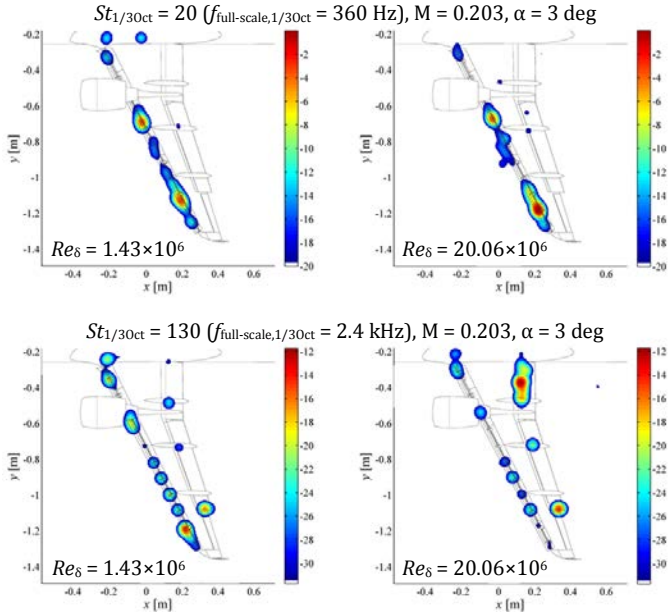

Fig. 2: Comparison of source maps at different Reynolds numbers.

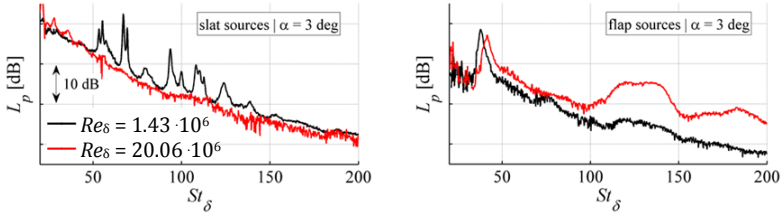

Fig. 3: Comparison of spectra at different Reynolds numbers (red).

In summary, several sources with a significant Reynolds number dependence were being shown. These include dominant sources on the flap at real flight Reynolds number and various peaks in the spectra with combined Strouhal and Reynolds number dependencies. The ability of measuring airframe noise at real flight Reynolds numbers now gives the possibility of separating the effect of the Reynolds number from the effects of model fidelity and Mach number on aeroacoustic behavior.

References

1. Ahlefeldt, T. “Microphone Array Measurement in European Transonic Wind Tunnel at Flight Reynolds Numbers,” AIAA Journal, Vol. 55, No. 1, 2017, pp. 36–48.
2. Ahlefeldt, T., and Koop, L., “Microphone Array Measurements in a Cryogenic Wind Tunnel,” AIAA Journal, Vol. 48, No. 7, 2010, pp. 1470–1479.
3. Ahlefeldt, T., “Aeroacoustic Measurements of a Scaled Half-Model at High Reynolds Numbers,” AIAA Journal, Vol. 51, No. 12, 2013, pp.2783–2791.
4. Spehr C., Ahlefeldt T., “Comparison of Microphone Array Measurements in the Closed Test Section of LSWT and ETW,” CEAS Aeronautical Journal, (forthcoming, accepted for publication 02-2018)
5. R.W. Stoker, R. W., Guo, Y. P., Street, G., and Burnside, N., “Airframe Noise Source Location of a 777 Aircraft in Flight and Comparisons with Past Model Scale Tests,” Ninth AIAA/CEAS Aeroacoustics Conference, AIAA Paper 2003-3232, 2003.
6. Quest, J., “ETW—High Quality Test Performance in Cryogenic Environment,” 21st Aerodynamic Measurement Technology and Ground Testing Conference, AIAA Paper 2000-2260, 2000
7. Ahlefeldt, T., and Quest, J., “High-Reynolds Number Aeroacoustic Testing Under Pressurised Cryogenic Conditions in PETW,” 50th AIAA Aerospace Sciences Meeting Including the New Horizons Forum and Aerospace Exposition, AIAA Paper 2012-0107, 2012
8. Sitsma, P., “Experimental Techniques for Identification and Characterisation of Noise Sources,” National Aerospace Lab. NLR Rept. NLRTP-2004-165, 2004
9. Sitsma, P., “CLEAN Based on Spatial Source Coherence,” International Journal of Aeroacoustics, Vol. 6, No. 4, 2007, pp. 357–374
10. Dobrzynski, W., “Almost 40 Years of Airframe Noise Research: What Did We Achieve?” Journal of Aircraft, Vol. 47, No. 2, 2010, pp. 353–367